

Charmless B decay measurements at Belle

Yun-Tsung Lai ^{a,*}

^a*Kavli IPMU, University of Tokyo, Kashiwa, Japan*

E-mail: yun-tsung.lai@ipmu.jp

In this report, we summarize the recent charmless B decay measurements at Belle. The studies are based on the Belle data sample of 711 fb^{-1} or 121 fb^{-1} collected at $\Upsilon(4S)$ or $\Upsilon(5S)$ resonance at the KEKB collider. Results of several decay modes are presented. In addition to their branching measurements, the structure in the two-body invariant mass are also investigated for some of the decay modes.

*11th International Workshop on the CKM Unitarity Triangle (CKM2021)
22-26 November 2021
The University of Melbourne, Australia*

*On behalf of the Belle Collaboration.

*Speaker

1. Introduction

Charmless B decays are suppressed in Standard Model (SM), and are also sensitive to physics beyond the Standard Model (BSM) within the loop of penguin amplitude. Precise measurements on them could be a good sensitivity test against the prediction by SM. The main experimental challenge is the signal rate which is about 10^5 times smaller than the $e^+e^- \rightarrow q\bar{q}$ ($q = u, d, s, c$) continuum processes. Reduction of combinatorial background is hence critical. Using a Belle data sample of 711 fb^{-1} or 121 fb^{-1} collected at $\Upsilon(4S)$ or $\Upsilon(5S)$ resonance with the Belle detector [1] at the KEKB asymmetric-energy e^+e^- collider [2], we report the studies of the following B and B_s^0 decay modes: $B^0 \rightarrow p\bar{p}\pi^+\pi^-$, $B^+ \rightarrow p\bar{p}\pi^+\pi^0$ [3], $B^+ \rightarrow K^+K^-\pi^+$, $B^+ \rightarrow \pi^+\pi^0\pi^0$, $B_s^0 \rightarrow \eta'X_{s\bar{s}}$ [4], $B_s^0 \rightarrow \eta'\eta$ [5], and $B_s^0 \rightarrow \eta'K_S^{0\pm}$. Their signal yields (N_{sig}) are measured by one or multi-dimensional extended unbinned likelihood fit on data with different variables, and branching fractions are estimated by $\mathcal{B} = \frac{N_{\text{sig}}}{\epsilon \times N_B}$, where ϵ is the signal reconstruction efficiency and N_B is the number of B events (772M for B^+ or B^0 , 16.6M for B_s^0).

2. $B^0 \rightarrow p\bar{p}\pi^+\pi^-$ and $B^+ \rightarrow p\bar{p}\pi^+\pi^0$

Baryonic B decays have various interesting features, such as the enhancement in the di-baryon low mass threshold [6], and the different angular distributions from different modes e.g. between $B^+ \rightarrow p\bar{p}K^+$ and $B^+ \rightarrow p\bar{p}\pi^+$ [7]. Signal B candidate is identified by the energy difference $\Delta E \equiv E_B - E_{\text{beam}}$ and the beam-energy-constrained mass $M_{\text{bc}} \equiv \sqrt{E_{\text{beam}}^2/c^4 - |p_B/c|^2}$, where E_{beam} is the beam energy, and p_B and E_B are the momentum and energy of the reconstructed B meson, respectively. We use 2D fit with ΔE and M_{bc} to extract N_{sig} , and obtain $\mathcal{B}(B^0 \rightarrow p\bar{p}\pi^+\pi^-) = (0.83 \pm 0.17(\text{stat.}) \pm 0.17(\text{syst.})) \times 10^{-6}$ and $\mathcal{B}(B^+ \rightarrow p\bar{p}\pi^+\pi^0) = (4.58 \pm 1.17(\text{stat.}) \pm 0.67(\text{syst.})) \times 10^{-6}$. The total measured $\mathcal{B}(B^+ \rightarrow p\bar{p}\pi^+\pi^0)$ is about a factor of 10 smaller than the predicted $\mathcal{B}(B^+ \rightarrow p\bar{p}\rho^+)$ from a theoretical calculation by generalized factorization method [8]. Figure 1 shows the $M_{\pi\pi}$ distribution. A χ^2 fit is performed on $M_{\pi^+\pi^0}$ and we obtain 86 ± 41 events for $B^+ \rightarrow p\bar{p}\rho^+$. Table 1 shows the signal yields in $M_{p\bar{p}}$ bins. Branching fraction of $B^0 \rightarrow p\bar{p}\pi^+\pi^-$ in the threshold enhancement region (the lowest bin) is estimated as $(0.35 \pm 0.13(\text{stat.}) \pm 0.07(\text{syst.})) \times 10^{-6}$, which is consistent with the LHCb result [9].

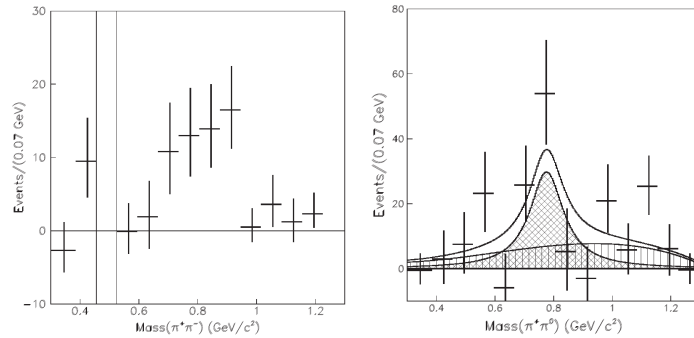


Figure 1: $M_{\pi^+\pi^-}$ (left) and $M_{\pi^+\pi^0}$ (right) distributions of $B^0 \rightarrow p\bar{p}\pi^+\pi^-$ and $B^+ \rightarrow p\bar{p}\pi^+\pi^0$, respectively.

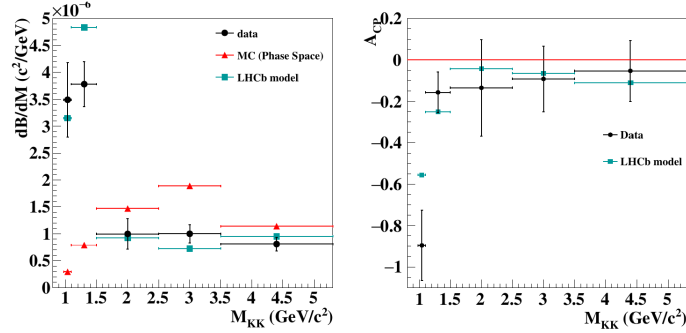
[†]Throughout this paper, inclusion of charge-conjugate decay modes is always implied.

Table 1: Fitted yields of $B^0 \rightarrow p\bar{p}\pi^+\pi^-$ ($0.6 \text{ GeV}/c^2 < M_{\pi^+\pi^-} < 1.22 \text{ GeV}/c^2$) and $B^+ \rightarrow p\bar{p}\pi^+\pi^0$ ($M_{\pi^+\pi^0} < 1.3 \text{ GeV}/c^2$) in $M_{p\bar{p}}$ bins.

$M_{p\bar{p}}$ (GeV/c^2)	Yield of $B^0 \rightarrow p\bar{p}\pi^+\pi^-$	Yield of $B^+ \rightarrow p\bar{p}\pi^+\pi^0$
$M_{p\bar{p}} < 2.85$	$26.1^{+10.0}_{-9.1}$	$133.5^{+26.6}_{-25.2}$
$2.85 < M_{p\bar{p}} < 3.128$	$19.6^{+10.2}_{-9.3}$	$12.3^{+10.3}_{-9.7}$
$3.128 < M_{p\bar{p}}$	$29.1^{+16.2}_{-13.1}$	$-3.8^{+15.1}_{-13.8}$

3. $B^+ \rightarrow K^+K^-\pi^+$

Compared to previous measurement by Belle [10], $B^+ \rightarrow K^+K^-\pi^+$ result is updated with a re-optimized binning to study the property of the structure and localized \mathcal{A}_{CP} at low $M_{K^+K^-}$ region which were also observed in BaBar [11] and LHCb [12–14]. Signal yields and \mathcal{A}_{CP} are extracted by using 2D fit with ΔE and M_{bc} within each $M_{K^+K^-}$ bins, and Figure 2 shows the results. The structure at $M_{K^+K^-} < 1.1 \text{ GeV}/c^2$ has an \mathcal{A}_{CP} of $-0.90 \pm 0.17(\text{stat.}) \pm 0.03(\text{syst.})$ with a significance of 4.8σ . Helicity angle (θ_{hel} , defined as the angle between B^+ and K^+ in the K^+K^- rest frame) for signal events within $M_{K^+K^-} < 1.1 \text{ GeV}/c^2$ is shown in Figure 3. The distribution is consistent with a coherent sum of spin-0 and spin-1 the most.

**Figure 2:** Differential branching fraction (left) and \mathcal{A}_{CP} (right) distributions as a function of $M_{K^+K^-}$ for $B^+ \rightarrow K^+K^-\pi^+$.

4. $B^+ \rightarrow \pi^+\pi^0\pi^0$

The major challenge in the $B^+ \rightarrow \pi^+\pi^0\pi^0$ measurement is the shower leakage [15] due to two π^0 in the reconstruction, and the correlation between energy and other variables. e.g. between ΔE and $M_{\pi\pi}$. To handle those effects, we require the momentum to be greater $0.5 \text{ GeV}/c^2$ for all π^0 candidates. By a 3D fit with ΔE , M_{bc} , and a Neural-Network [16] output discriminant for continuum suppression [17], we obtain inclusive $\mathcal{B}(B^+ \rightarrow \pi^+\pi^0\pi^0) = (19.0 \pm 1.5(\text{stat.}) \pm 1.4(\text{syst.})) \times 10^{-6}$ and $\mathcal{A}_{CP} = (9.2 \pm 6.8(\text{stat.}) \pm 0.5(\text{syst.}))\%$. We use the $s\mathcal{P}lot$ technique [18] to isolate signal on $M_{\pi\pi}$ distribution, and perform a 2D binned fit on the histogram to extract the signal model composition as shown in Figure 4. In addition to the $B^+ \rightarrow \rho(770)^+\pi^0$ structure at low $M_{\pi^+\pi^0, \text{min}}$

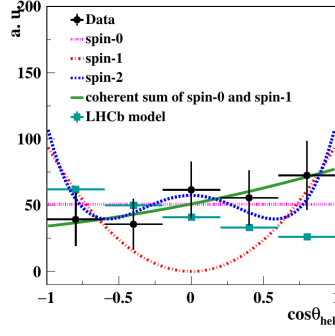


Figure 3: The helicity angle distribution with applying efficiency correction and comparisons to different models, where the LHCb model is from Ref. [13].

region[†], and we also observe a new structure at $M_{\pi^0\pi^0}$ region, which is modeled by an incoherent sum of $f_0(980)$, $f_2(1270)$, and $f_0(500)$. A combined branching fraction for this $\pi^0\pi^0$ structure is measured as $(6.9 \pm 0.9(\text{stat.}) \pm 0.6(\text{syst.})) \times 10^{-6}$, which has a significance of 9.2σ . A large \mathcal{A}_{CP} is seen at $M_{\pi^0\pi^0} \sim 1.4 \text{ GeV}/c^2$ as shown in Figure 5.

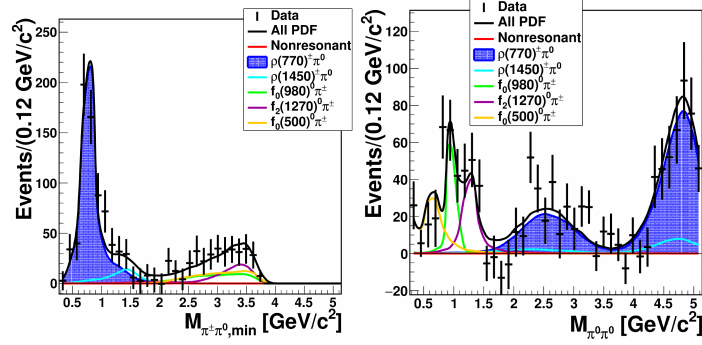


Figure 4: Projection of the fit result to s -Weights $M_{\pi^+\pi^0,\min}$ -vs- $M_{\pi^0\pi^0}$ histogram.

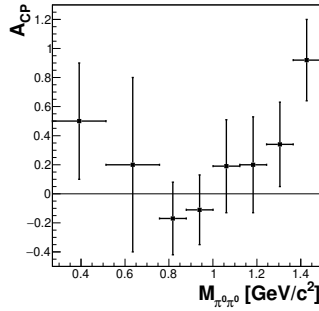


Figure 5: s -Weights \mathcal{A}_{CP} as a function of $M_{\pi^0\pi^0}$ for $M_{\pi^+\pi^0,\min} > 1.9 \text{ GeV}/c^2$. The first few bins are combined due to low number of events.

[†] $M_{\pi^+\pi^0,\min}$ refers to the smaller of two $M_{\pi^+\pi^0}$ values in a reconstructed B candidate.

5. $B_s^0 \rightarrow \eta' X_{s\bar{s}}, B_s^0 \rightarrow \eta' \eta$, and $B_s^0 \rightarrow \eta' K_S^0$

As B decays with η' in the final state have been observed firstly by CLEO [19, 20], we have found some special properties in this particle and decays involving it. η' mass is higher than the expectation from symmetry considerations [21]. Measurements of $\mathcal{B}(B \rightarrow \eta' X_s)$ [23–25] also show unexpected enhancement compared with SM prediction [22]. Any new observation on decays with η' could provide further information to understand its property.

We report the first measurement on $B_s^0 \rightarrow \eta' X_{s\bar{s}}$ based on a semi-inclusive method [4]. Simulation of $X_{s\bar{s}}$ fragmentation is performed with PYTHIA 6 [26] with a flat mass distribution. $X_{s\bar{s}}$ candidates are reconstructed with two kaons (K^+K^- or $K^\pm K_S^0$ with $K_S^0 \rightarrow \pi^+\pi^-$) and up to four pions with at most one π^0 . η' candidates are reconstructed with $\pi^+\pi^-\eta$ and $\eta \rightarrow \gamma\gamma$. N_{sig} is extracted by a 1D fit on M_{bc} with $-0.12 \text{ GeV} < \Delta E < 0.05 \text{ GeV}$ in $M_{X_{s\bar{s}}}$ bins. As none of the bins shows significant yield, we set an upper limit on $\mathcal{B}(B_s^0 \rightarrow \eta' X_{s\bar{s}})$ as 1.4×10^{-3} at 90% confidence level (C.L.).

Branching fraction and CP asymmetry of $B_s^0 \rightarrow \eta' \eta$ decay could be affected by various BSM scenarios [28]. Along with the results of other $B_{d,s}^0 \rightarrow \eta\eta, \eta'\eta, \eta'\eta'$ modes, measurement on $B_s^0 \rightarrow \eta'\eta$ is helpful to extract CP -violating parameters from SU(3)/U(3) symmetry [29]. N_{sig} of $B_s^0 \rightarrow \eta'\eta$ is extracted by 3D fit with ΔE , M_{bc} , and $M_{\eta'}$. We obtain 2.7 ± 2.5 events and set upper limits of $f_s \times \mathcal{B}(B_s^0 \rightarrow \eta'\eta)$ and $\mathcal{B}(B_s^0 \rightarrow \eta'\eta)$ as 1.3×10^{-5} and 6.5×10^{-5} at 90% C.L., respectively, where f_s is the fraction of $B_s^{(*)0} \bar{B}_s^{(*)0}$ in $b\bar{b}$ events and its world average is 0.201 ± 0.031 [27].

$B_s^0 \rightarrow \eta' K_S^0$ decay contains contributions from gluonic and electroweak penguin amplitudes, such that it is sensitive to BSM physics [28] which can affect both decay rate and CP asymmetries. N_{sig} of $B_s^0 \rightarrow \eta' K_S^0$ is extracted by 3D fit with ΔE , M_{bc} , and $M_{\eta'}$. We obtain -3.21 ± 1.85 events and set upper limits of $f_s \times \mathcal{B}(B_s^0 \rightarrow \eta' K_S^0)$ and $\mathcal{B}(B_s^0 \rightarrow \eta' K_S^0)$ as 1.64×10^{-5} and 8.16×10^{-5} at 90% C.L., respectively.

6. Summary

We report the results of several charmless B decays using Belle data collected at $\Upsilon(4S)$ or $\Upsilon(5S)$ resonance. In addition to branching fraction measurement, we also look into the distribution of two-body invariant mass of $B^0 \rightarrow p\bar{p}\pi^+\pi^-$, $B^+ \rightarrow p\bar{p}\pi^+\pi^0$, $B^+ \rightarrow K^+K^-\pi^+$, and $B^+ \rightarrow \pi^+\pi^0\pi^0$ to study their decay structure. We do not observe significant signal yield for $B_s^0 \rightarrow \eta' X_{s\bar{s}}$, $B_s^0 \rightarrow \eta'\eta$, and $B_s^0 \rightarrow \eta' K_S^0$, and upper limits on branching fraction are estimated at 90% C.L.. In near future, larger data set from Belle II [30] can further improve the measurement on these decay modes.

References

- [1] A. Abashian *et al.* (Belle Collaboration), Nucl. Instrum. Methods Phys. Res., Sect. A **479**, 117 (2002); also see detector section in J. Brodzicka *et al.*, Prog. Theor. Exp. Phys. **2012**, 04D001 (2012).
- [2] S. Kurokawa and E. Kikutani, Nucl. Instrum. Methods Phys. Res., Sect. A **499**, 1 (2003), and other papers included in this volume; T. Abe *et al.*, Prog. Theor. Exp. Phys. **2013**, 03A001 (2013) and references therein.

- [3] K. Chu *et al.* (Belle Collaboration), Phys. Rev. D **101**, 052012 (2020).
- [4] S. Dubey *et al.* (Belle Collaboration), Phys. Rev. D **104**, 012007 (2021).
- [5] N.K. Nisar *et al.* (Belle Collaboration), Phys. Rev. D **104**, L031101 (2021).
- [6] K. Abe *et al.* (Belle Collaboration), Phys. Rev. Lett. **88**, 181803 (2002).
- [7] J. Wei *et al.* (Belle Collaboration), Phys. Lett. B **659**, 80 (2008).
- [8] C. Q. Geng, Y. K. Hsiao, and J. N. Ng, Phys. Rev. D **75**, 094013 (2007).
- [9] R. Aaij *et al.* (LHCb Collaboration), Phys. Rev. D **96**, 051103 (2017).
- [10] C.-L. Hsu *et al.* (Belle Collaboration), Phys. Rev. D **96**, 031101(R) (2017).
- [11] B. Aubert *et al.* (BaBar Collaboration), Phys. Rev. Lett. **99**, 221801 (2017).
- [12] R. Aaij *et al.* (LHCb Collaboration), Phys. Rev. Lett. **112**, 011801 (2014).
- [13] R. Aaij *et al.* (LHCb Collaboration), Phys. Rev. Lett. **123**, 231802 (2019).
- [14] R. Aaij *et al.* (LHCb Collaboration), Phys. Rev. Lett. **112**, 011801 (2014).
- [15] K. Miyabayashi, Nucl. Instrum. Methods Phys. Res., Sect. A **494**, 298 (2002).
- [16] M. Feindt and U. Kerzel, Nucl. Instrum. Methods Phys. Res., Sect. A **559**, 190 (2006).
- [17] G. C. Fox and S. Wolfram, Phys. Rev. Lett. **41**, 1581 (1978). The modified moments used in this paper are described in S. H. Lee *et al.* (Belle Collaboration), Phys. Rev. Lett. **91**, 261801 (2003).
- [18] M. Pivk and F. R. Le Diberder, Nucl. Instrum. Methods Phys. Res., Sect. A **555**, 356 (2005).
- [19] T.E. Browder *et al.* (CLEO Collaboration), Phys. Rev. Lett., **81**, 1786, 1998.
- [20] G. Bonvicini *et al.* (CLEO Collaboration), Phys. Rev. D, **68**, 011101, 2003.
- [21] K. Ottnad and C. Urbach (ETM Collaboration), Phys. Rev. D **97**, 054508 (2018).
- [22] A. Datta, X.-G. He, and S. Pakvasa, Phys. Lett. B **419**, 369 (1998).
- [23] G. Bonvicini *et al.* (CLEO Collaboration), Phys. Rev. D **68**, 011101 (2003).
- [24] B. Aubert *et al.* (BABAR Collaboration), Phys. Rev. Lett. **93**, 061801 (2004).
- [25] K. Nishimura *et al.* (Belle Collaboration), Phys. Rev. Lett. **105**, 191803 (2010).
- [26] T. Sjostrand, S. Mrenna, and P. Skands, J. High Energy Phys. **06** 026 (2006).
- [27] P. A. Zyla *et al.* (Particle Data Group), Prog. Theor. Exp. Phys. **2020**, 083C01 (2020).
- [28] E. Kou *et al.*, Prog. Theor. Exp. Phys. 123C01 (2019).
- [29] Y.-K. Hsiao, C.-F. Chang, and X.-G. He, Phys. Rev. D **93**, 114002 (2016).
- [30] T. Abe *et al.* (Belle II Collaboration), arXiv:1011.0352 [physics.ins-det], (2010).